The electronic structure of the PtH molecule

Visscher, L.; Saue, T.; Nieuwpoort, W. C.; Faegri, K.; Gropen, O.

Published in:
Journal of Chemical Physics

DOI:
10.1063/1.465813

The electronic structure of the PtH molecule: Fully relativistic configuration interaction calculations of the ground and excited states

L. Visscher, T. Saue, W. C. Nieuwpoort, K. Faegri, and O. Gropen

Citation: The Journal of Chemical Physics **99**, 6704 (1993); doi: 10.1063/1.465813
View online: https://doi.org/10.1063/1.465813
View Table of Contents: http://aip.scitation.org/toc/jcp/99/9
Published by the American Institute of Physics

The electronic structure of the PtH molecule: Fully relativistic configuration interaction calculations of the ground and excited states

L. Visscher
Department of Chemical Physics and Material Science Centre, University of Groningen, Nijenborgh 4, 9747 AG Groningen, The Netherlands

T. Saue
Department of Chemistry, University of Oslo, P.O. Box 1033 Blindern, 0315 Oslo 3, Norway

W. C. Nieuwpoort
Department of Chemical Physics and Material Science Centre, University of Groningen, The Netherlands

K. Faegri
Department of Chemistry, University of Oslo, P.O. Box 1033 Blindern, 0315 Oslo 3, Norway

O. Gropen
Institute of Mathematical and Physical Sciences, University of Tromsø, 9000 Tromsø, Norway

(Received 10 June 1993; accepted 12 July 1993)

Fully relativistic all-electron self-consistent field calculations based on the Dirac–Coulomb Hamiltonian have been performed on the three lowest lying states of the PtH molecule. The resulting four-component Dirac–Hartree–Fock (DHF) molecular spinors are subsequently used in relativistic configuration interaction (CI) calculations on the five lower states of PtH. Spectroscopic properties are obtained by fitting the potential curve to a Morse function and show good agreement with experimental data. The effect of relativistic corrections to the Coulomb electron–electron interaction is investigated at the DHF level and is found to be insignificant for the molecular spectroscopic properties investigated by us. The CI wave functions are found to have only one dominant configuration, indicating a lack of static correlation. Dynamic correlation in the *d* shell is, however, important for the spectroscopic properties of PtH. The results conform with a bonding scheme in which the three lower and two upper states of PtH are assigned $5d^4_{3/2}5d^5_{5/2}\sigma^2_{1/2}$ and $5d^3_{3/2}5d^6_{5/2}\sigma^2_{1/2}$ electronic configurations, respectively. The configurations are only approximate and are perturbed by $5d$ participation in bonding. The stability of the Pt–H bond is explained in terms of the relativistic stabilization of the $6s$ orbital in analogy with the electron affinity of the platinum atom.

I. INTRODUCTION

The catalytic versatility of platinum makes it one of the most widely applied metal catalysts.[1] A number of the reactions for which platinum is active involves hydrogen. This has motivated extensive research on the nature of the platinum–hydrogen bonding. Platinum hydride offers the simplest example of the platinum–hydrogen bond and this open-shell molecule has therefore been the subject of several studies, most of them *ab initio* calculations.[2–8]

Platinum being a third row transition metal, both correlation and relativistic effects are expected to be of importance in its chemistry.[9] Transition-metal atoms, in general, are characterized by the close proximity of nd, $(n+1)s$, and $(n+1)p$ orbitals which gives rise to an abundance of low-lying atomic states with strong configurational mixing. Proper handling of static correlation is therefore a prerequisite for the correct description of the atomic spectra. With an increasing number of d electrons dynamic correlation becomes more and more significant. At the molecular level these features give rise to a number of possible bonding mechanisms and may lead to complicated molecular spectra. An additional complicating factor for third row transition metals in particular is that relativistic effects may significantly influence bonding and spectroscopic properties.[10] Spin–orbit effects in the platinum atom give a splitting of the order of 10 000 cm^{-1} for the $^3D(5d^96s^1)$ state while the singlet–triplet splitting for this configuration is only 3800 cm^{-1}. The relativistic contraction of the $6s$ orbital and the expansion of the $5d$ shell will influence the bonding and change the character of the bonding orbitals.

In the majority of *ab initio* calculations on PtH relativistic effects are introduced through the use of relativistic effective core potentials (RECP's) (Ref. 11) an approach which also yields significant reduction of computational effort relative to all-electron calculations. Effective core potentials replace the core electrons under the assumption that the core remains frozen during bond formation. RECP's may be obtained by fitting the potential to a fully relativistic atomic calculation or alternatively a semirelativistic calculation such as the Cowan Griffin method[12] or the second-order Douglas–Kroll ("no-pair") approximation.[13] In general, some averaging procedure is employed to generate spin-free RECP's. The RECP approach has the advantage of staying within the nonrelativistic theoretical framework so that most computational methods and computer codes for nonrelativistic calculations may be used with little or no modification. Spin–orbit effects may be introduced by adding spin–orbit matrix elements to the

 0021-9606/93/99(9)/6704/12/$6.00

Hamiltonian matrix of *LS*-coupled states connected through the spin–orbit operator. The disadvantage of the RECP method is that the fitting and averaging procedure introduces uncertainities and that the quality of the RECP may be difficult to assess without performing all-electron atomic and molecular calibration calculations at the same level of approximation.

An alternative approach is to solve the relativistic Dirac–Hartree–Fock (DHF) equations.[14] This will generate four-component spinors which provide a natural description of the relativistic effects. The disadvantage of this approach is mainly the large computer resources necessary to carry out four-component relativistic calculations. Over the past few years, however, a number of DHF molecular codes and results[15–19] have been reported. Recently Dyall[8] presented results from DHF calculations on platinum hydrides, including PtH. The next step towards a quantitatively correct description of heavy atoms like platinum is to include electron correlation in the formalism and go beyond the mean field approach. The molecular spinor basis generated by the DHF method may be used to generate many-electron (determinantal) wave functions with which one can expand the configuration interaction (CI) equations in a completely relativistic framework.

In this work we present the results of fully relativistic CI calculations of the five lowest states of the PtH molecule and compare the result with other methods and with experiment. In the following we give a brief introduction to the computational methods used by us. We then discuss the atomic aspects of calculations on PtH before presenting results from molecular DHF and CI calculations.

II. COMPUTATIONAL METHODS

We have performed CI calculations using references obtained from DHF calculations. Below a short resumé of the DHF method is given followed by a description of the CI method recently developed by one of us (L.V.). Unless otherwise stated all calculations have been performed using the MOLFDIR program package.[20]

A. The DHF method

The starting point of our calculations is the Dirac–Coulomb equation

$$H\Psi=E\Psi, \tag{1}$$

$$H=\sum_{i}^{N} h_i+\sum_{i<j} g_{ij}, \tag{2}$$

where h is the one-electron Dirac Hamiltonian

$$h=\begin{bmatrix} V\cdot I_2 & c(\sigma\cdot\mathbf{p}) \\ c(\sigma\cdot\mathbf{p}) & (V-2c^2)\cdot I_2 \end{bmatrix} \tag{3}$$

I_2 and σ are the 2×2 identity and Pauli matrices respectively, while the potential V describes the interaction of the electrons with the fixed nuclear framework. A detailed description of this Hamiltonian may be found in standard textbooks.[21,22] The electron–electron interaction, g_{ij}, is given by the Coulomb operator

$$g_{ij}=\frac{1}{r_{ij}} \tag{4}$$

and represents in this context the zeroth-order approximation to the full relativistic electron–electron interaction. A first order correction is provided by the Breit operator,[23] which may be split[24] into a magnetic part, usually termed the Gaunt interaction,[25] and a retardation part.

$$g_{ij}^{\text{Breit}}=-\frac{(\alpha_i\cdot\alpha_j)}{r_{ij}}-\frac{(\alpha_i\cdot\nabla_i)(\alpha_j\cdot\nabla_j)r_{ij}}{2}$$

$$=g_{ij}^{\text{Gaunt}}+g_{ij}^{\text{retardation}}. \tag{5}$$

Our computer program allows for the inclusion of the Gaunt interaction either in a variational or in a perturbative scheme.

From the Dirac–Coulomb equation open-shell DHF equations can be derived in the same way as the nonrelativistic Hartree–Fock equations.[26] By minimizing the (averaged) energy expression of a system with one open shell, we get the following set of equations

$$F^C=h+Q^C+Q^O+\alpha L^O, \quad F^O=h+Q^C+aQ^O+\alpha L^C, \tag{6}$$

$$Q^C=\sum_k J_k-K_k, \quad Q^O=f\sum_m J_m-K_m, \tag{7}$$

$$L^C=\sum_k L_k, \quad L^O=f\sum_m L_m, \tag{8}$$

$$J_i|j\rangle=\langle i|g_{12}|i\rangle\,|j\rangle, \quad K_i|j\rangle=\langle i|g_{12}|j\rangle\,|i\rangle, \tag{9}$$

$$L_i|j\rangle=\langle i|Q^O|j\rangle\,|i\rangle+\langle i|j\rangle Q^O|i\rangle. \tag{10}$$

In these equations k and m are used to label closed- and open-shell molecular four spinors, respectively. The fractional occupation number (f) of the open-shell spinors and the coupling coefficients (a and α) are defined by the number of open-shell electrons (n) and the number of open-shell spinors (m)

$$f=\frac{n}{m}, \quad a=\frac{m(n-1)}{n(m-1)}, \quad \alpha=\frac{1-a}{1-f}. \tag{11}$$

The DHF equations are expanded in a Gaussian type basis set. This basis set is made up of two subsets describing the upper (large) components and the lower (small) components of the spinors. In order to get a correct representation of all operators these bases are chosen to be related by the kinetic or atomic balance relation.[27] For open-shell systems the average of configuration energy is minimized after which the energies of individual states can be obtained by complete open-shell configuration interaction[28] (COSCI)—diagonalization of the CI matrix of all possible configurations in the open-shell manifold.

B. The relativistic CI method

We have developed a relativistic version of the restricted active space configuration interaction[29] (RASCI) method which can be used to improve the wave functions and energy differences found in the DHF (COSCI) step.

In the restricted active space method the active spinor space is divided in three groups. The first group (RAS1) contains the highest occupied closed-shell spinors of the reference determinant(s). The second group (RAS2) contains the open-shell spinors of the reference determinant(s). The spinors that were unoccupied in the reference determinant(s) are in the third group (RAS3). The CI space is now defined by specifying a maximum excitation level (n_{H1}) from RAS1 and a maximum excitation level (n_{E3}) to RAS3. Determinants that fulfill the constraint of having n_{H1}, or less, holes in RAS1 and n_{E3}, or less, electrons in RAS3 form the CI space. This definition allows most of the conventional types of CI to be done as a special case.

To describe the method it is convenient to write the Dirac–Coulomb–(Gaunt) Hamiltonian in second quantized form. Using the generators of the unitary group $E_{ij}=a_i^+ a_j$, the Hamiltonian can be written as

$$H=\sum_{i,j}\langle i|h|j\rangle E_{ij}+\frac{1}{2}\sum_{i,j,k,l}(ij|g|kl)(E_{ij}E_{kl}-E_{il}\delta_{jk}). \tag{12}$$

In this equation molecular spinors are labeled by i and j. The summation is restricted to the electron solutions, since we neglect any (virtual) positron–electron pair creation. We expand the many-electron wave functions in the determinantal basis $\{\Phi_I\}$ defined earlier. The result is a matrix representation of the Hamiltonian which can be expressed as a sum of one- and two-electron integrals multiplied by coupling constants γ_{ij}^{IJ} and Γ_{ijkl}^{IJ}, respectively,

$$\mathbf{H}_{IJ}=\sum_{i,j}h_{ij}\gamma_{ij}^{IJ}+\sum_{i,j,k,l}(ij|kl)\Gamma_{ijkl}^{IJ} \tag{13}$$

with $h_{ij}=\langle i|h|j\rangle$, $(ij|kl)=(ij|g|kl)$, $\gamma_{ij}^{IJ}=\langle I|E_{ij}|J\rangle$, and $\Gamma_{ijkl}^{IJ}=\frac{1}{2}\langle I|E_{ij}E_{kl}-E_{il}\delta_{jk}|J\rangle$.

Since the matrix, in general, will be too large to hold in memory, we use the direct diagonalization technique of Davidson[30] to find the desired roots. The main difference with nonrelativistic direct CI methods is that the number of relativistic integrals is about 2^4 times as large since each molecular orbital corresponds to two molecular spinors. Another complication is that the integrals in general will be complex since the Hamiltonian contains complex operators. Thus the number of virtual spinors and the number of determinants that can be used is smaller than what is presently possible with efficient nonrelativistic CI methods. Our direct RASCI code can at present handle expansions up to about 200 000 determinants using an active spinor space of about 100 spinors. In the present application a number of high-lying virtual spinors were deleted to make the calculations feasible.

III. ATOMIC CALCULATIONS

The classification of some of the observed lines in the platinum atomic optical spectrum was done already in 1927 and a review of the assigned lines can be found in Moore's tables.[31] The ground state of the platinum atom is a $J=3$ state designated $^3D_3$. The first two states arise mainly from the $5d^9(^2D_{5/2})6s^1$ configuration and the seventh and eighth states from the $5d^9(^2D_{3/2})6s^1$ configuration. The atomic spectrum is complicated because the configurations d^9s^1 and d^8s^2 are close in energy and the individual states mix strongly with each other due to the strong spin–orbit coupling.[8] This makes the assignment of *LS*-coupling term symbols rather arbitrary and we shall use instead the J value and parity to designate the states. In the following we describe the basis set used in the molecular calculations and compare finite basis DHF results with corresponding numerical results for an estimate of the sensitivity to basis set errors. We then discuss results obtained at different levels of theory and compare them with the experimental (spectroscopic) data of the Pt atom. The relativistic optimization of single exponents and all the numerical calculations were done using the GRASP atomic structure code.[32]

A. Basis sets

The platinum basis was derived from a nonrelativistically optimized $22s16p13d8f$ Gaussian basis[33] (basis I). Due to the relativistic contraction of s and p orbitals a relativistic reoptimization of the basis would be expected to give a shift towards higher exponents in the basis. We have not done this explicitly, but found that inclusion of a relativistically optimized p function with exponent $7.9E5$ gave an improvement of 827 mH in the total energy (see also Ref. 34). No tight s exponent was needed, due to our use of a finite nucleus model[35] (a Gaussian charge distribution with exponent $0.12E9$). This large (L) component primitive basis was subjected to general contraction using the coefficients from an atomic DHF calculation and augmented with diffuse correlation and polarization functions. Due to the relativistic contraction of p orbitals, the outer p exponent in the primitive basis mainly describes the $6p$ orbital and it was thus sufficient to add only one diffuse relativistically optimized p function to obtain a double-zeta description of this orbital. The basis was furthermore supplemented with one d function and one f function, the latter contracted from three primitives.[36] The small (S) component contracted basis was generated using the atomic balance relation.[37] For both basis subsets different contraction coefficients were used for spinors that differ by their j value, but an overlap criterion was used to reduce the resulting number of contracted functions. The final $[8s10p9d3f(L)|6s13p12d11f4g(S)]$ basis (basis II) was used in the subsequent atomic and molecular calculations. The two different basis sets are compared in Table I.

For hydrogen a primitive $6s1p$ Gaussian basis was relativistically contracted to $3s1p$. The hydrogen basis set is given in Appendix A. The atomic energy is $-0.499\,952$ H, differing from the numerical energy by 55 μH. The size of all basis sets is summarized in Table II.

B. The atomic spectrum

The first 12 lines in the platinum atomic spectrum arise from the $5d^86s^2$, $5d^96s^1$, and $5d^{10}$ configurations. In principle, the excitation energies can be calculated by performing a full CI within this configurational space. However, it is difficult to find a one-particle basis which describes all con-

TABLE I. Total and orbital energies (in Hartrees) from numerical and finite basis DHF calculations on the $5d_{3/2}^4(5d_{5/2},6s_{1/2})^6$ configurational average of the platinum atom.

	Numerical DF	Basis I	Basis II
Total energy	−18 434.181 187	−18 433.181 171	−18 434.007 850
$\epsilon(1s_{1/2})$	−2899.6195	−2899.6450	−2899.6270
$\epsilon(2s_{1/2})$	−514.7000	−514.7116	−514.7124
$\epsilon(2p_{1/2})$	−492.3144	−492.0991	−492.2879
$\epsilon(2p_{3/2})$	−428.6614	−428.6741	−428.6756
$\epsilon(3s_{1/2})$	−123.3795	−123.3897	−123.3926
$\epsilon(3p_{1/2})$	−113.3776	−113.3291	−113.3805
$\epsilon(3p_{3/2})$	−99.1889	−99.2001	−99.2024
$\epsilon(3d_{3/2})$	−82.7461	−82.7547	−82.7560
$\epsilon(3d_{5/2})$	−79.7133	−79.7237	−79.7262
$\epsilon(4s_{1/2})$	−27.8662	−27.8868	−27.8774
$\epsilon(4p_{1/2})$	−23.5882	−23.5944	−23.5968
$\epsilon(4p_{3/2})$	−20.1647	−20.1877	−20.1754
$\epsilon(4d_{3/2})$	−13.1548	−13.1556	−13.1642
$\epsilon(4d_{5/2})$	−12.5010	−12.4992	−12.5110
$\epsilon(4f_{5/2})$	−3.4763	−3.4963	−3.4855
$\epsilon(4f_{7/2})$	−3.3387	−3.3596	−3.3475
$\epsilon(5s_{1/2})$	−4.4622	−4.4793	−4.4667
$\epsilon(5p_{1/2})$	−3.0409	−3.0527	−3.0445
$\epsilon(5p_{3/2})$	−2.4255	−2.4410	−2.4292
$\epsilon(5d_{3/2})$	−0.4970	−0.4902	−0.4997
$\epsilon(5d_{5/2})$	−0.4191	−0.4178	−0.4216
$\epsilon(6s_{1/2})$	−0.3080	−0.3062	−0.3084
DHF+Breit	−18 413.910 101	DHF+Gaunt	−18 410.843 679

figurations in a balanced way. It has been pointed out by Hay[38] that orbitals of first-row transition metal atoms vary appreciably from one valence state to another. This also holds true for the platinum atom. Radial expectation values of the lower $J=0$, 2, 3, 4 atomic states from numerical DHF calculations are presented in Table III. We see that they may differ by as much as 0.5 bohr. As a further complication, the $5d^8 6s^2$ configuration will be biased in an optimization of spinors for the total energy average of all states arising from the three configurations, since this configuration gives rise to the majority of these states. A numerical calculation based on this spinor set therefore gives a $J=4$ ($5d^8 6s^2$) ground state which is not in agreement with experiment. A better choice for one spinor set to describe all configurations is the relativistic configurational average of the $5d_{3/2}^4 5d_{5/2}^4 6s_{1/2}^2$, $5d_{3/2}^4 5d_{5/2}^5 6s_{1/2}^1$, and $5d_{3/2}^4 5d_{5/2}^6 6s_{1/2}^0$ configurations. This average yields spinors that are most suitable for the low-lying states and will describe $d^8 s^2$ and $d^9 s^1$ states about equally well, but with the d^{10} state somewhat high.

We have performed both numerical and finite basis DHF atomic calculations using the latter relativistic average. The resulting spinors were used in COSCI calculations to obtain the energy of individual atomic states. The finite basis calculations were performed in O_h double group symmetry. The results of the DHF and COSCI calculations are presented in Tables I and IV, respectively. The total DHF energy obtained with the finite basis is 173 mH above the numerical limit while the differences in the COSCI spectrum indicate that the basis set is accurate to about 0.02 eV in the description of atomic splittings.

The finite basis results as well as the numerical results in Table IV show rather poor agreement with experiment. There are a number of possible reasons for these discrepancies. One of these is the neglect of correlation effects which are expected to be important. We therefore performed a somewhat larger CI calculation with the finite basis method. The number of high lying virtuals neglected in the atomic CI was the same as in the subsequent molecular calculations (70) in order to facilitate the evaluation of molecular dissociation energies. We included the $5d_{3/2}$, $5d_{5/2}$, and $6s_{1/2}$ spinors in the RAS2 space and 60 virtual spinors in the RAS3 space. The CI was then set up to allow all single and double excitations from ten electrons in the $(5d_{3/2},5d_{5/2},6s_{1/2})$ manifold giving an expansion of 889 416 determinants, which is reduced by symmetry to 111 646.

TABLE II. Basis set sizes.

	Large component		Small component	
	Primitive	Contracted	Primitive	Contracted
Pt basis I	22*s*16*p*13*d*8*f*		16*s*22*p*16*d*13*f*8*g*	
Pt basis II	22*s*18*p*14*d*11*f*	8*s*10*p*9*d*3*f*	18*s*22*p*21*d*14*f*11*g*	6*s*13*p*12*d*11*f*4*g*
H basis	6*s*1*p*	3*s*1*p*	1*s*6*p*1*d*	1*s*3*p*1*d*

TABLE III. Radial expectancies (bohr) of the lower $J=0$, 2, 3, 4 states of platinum. Nonrelativistic results have been obtained by scaling the speed of light by a factor of 1000.

Relativistic	$J=0$	$J=2$	$J=3$	$J=4$
$5d$	1.665	1.608	1.611	1.561
$5d$	1.778	1.693	1.703	1.629
$6s$	2.469	3.094	3.098	3.004
Nonrelativistic	d^{10}	d^9s^1		d^8s^2
$5d$	1.694	1.615		1.549
$6s$	2.366	3.708		3.546

The results should have approximately the same precision as the molecular results. These CI calculations (Table IV) give the right order of the three lowest states, although the magnitude of the splittings is still not correct. The correlation energy for the ground state was found to be 233 mH.

Another possible cause of disagreement with experiment is the neglect of relativistic corrections to the Coulomb electron–electron interaction. We have estimated the Gaunt and Breit corrections from perturbation theory. The results are not strictly commensurate since the first (Gaunt only) calculation was done in the finite basis set approach and the other (Breit) was done with the numerical GRASP code. The corrected DHF energies in Table I indicate, however, that the Gaunt correction forms the major contribution to the Breit correction. As seen from Table IV, at the COSCI level the trends in the Breit corrected splitting are very well represented with the Gaunt only calculation and we therefore conclude that the Gaunt only approach is accurate enough for our purposes. The effect of the Gaunt interaction on the atomic spectrum of platinum is of the same order as the CI corrections and the influence of both on molecular properties should therefore be considered.

From our atomic calculations we draw the conclusion that it is difficult to obtain a quantitatively correct description of the platinum atomic spectrum. The Breit (or Gaunt) interaction as well as correlation effects should be accounted for. In our atomic calculations basis set deficiencies appear to be small compared to the other sources of errors.

IV. MOLECULAR CALCULATIONS

In a simple approach to PtH within a nonrelativistic framework (Hunds case a) the Pt–H bond may be regarded as a $\sigma(s-s)$ bond arising from the platinum d^9s^1 configuration. According to Mulliken[39] the electronic structure of most diatomic hydrides may be accounted for by assuming that the electrons of the heavier atom retain their n,l, quantum numbers in the molecule and furthermore have a definite $\lambda=|m_l|$ value imposed by the strong axial electric field of the hydrogen nucleus. The electronic configuration of PtH may then be given as $5d^9\sigma^2$ and will give rise to three states, characterized by $\Lambda=|M_L|$ and $\Sigma=|M_S|$, in the order $^2\Delta < {}^2\Pi < {}^2\Sigma$ with $^2\Delta$ as the ground state, provided that the bonding orbital has the same character in all three states. The splitting between the three states will depend chiefly on the splitting of the nonbonding d orbitals in the axial field of the hydrogen atom.

The analogous approach within the fully relativistic framework (Hunds case c) first considers the spin–orbit splitting on the platinum atom, that splits the $5d$ shell into a $5d_{3/2}$ and a $5d_{5/2}$ shell. The configurations $5d^4_{3/2}5d^5_{5/2}\sigma^2_{1/2}$ and $5d^3_{3/2}5d^6_{5/2}\sigma^2_{1/2}$ give two groups of states that can be characterized by their $\Omega=|M_J|$ value. The lower group (1) of three states arises from the $5d^4_{3/2}5d^5_{5/2}\sigma^2_{1/2}$ configuration and will be in the order $\frac{5}{2}(1)<\frac{3}{2}(1)<\frac{1}{2}(1)$ with $\Omega=\frac{5}{2}$ as the ground state. The upper group (2) has the two states arising from the $5d^3_{3/2}5d^6_{5/2}\sigma^2_{1/2}$ configuration in the order $\frac{3}{2}(2)<\frac{1}{2}(2)$. With the platinum $5d$ orbitals so close in energy to the hydrogen s orbital this simple bonding picture may be perturbed by d participation in the bond, a feature that will mainly change the relative position of $\Omega=\frac{1}{2}$ states in the spectrum.

The two bonding schemes and their predicted spectra (sketched in Fig. 1) are connected by the spin–orbit interaction which splits the three $\Lambda\Sigma$ states into $^2\Sigma_{1/2}$, $^2\Pi_{1/2}$, $^2\Pi_{3/2}$, $^2\Delta_{3/2}$, and $^2\Delta_{5/2}$ states. The strong spin–orbit cou-

TABLE IV. Spectrum of the platinum atom. Figures in electronvolts, relative to the $J=3$ ground state.

	J Parity	Experiment (Ref. 9)		Num. DHF	Basis set DHF	Num. DHF+B	Basis set DHF+G	Basis set CI
1	3^+	$^2D_{5/2}\otimes{}^2S$	0.000	0.000	0.000	0.000	0.000	0.000
2	2^+	$^2D_{5/2}\otimes{}^2S$	0.096	0.159	0.163	0.145	0.146	0.145
3	4^+	$^3F_4$	0.102	0.095	0.116	0.039	0.045	0.262
4	0^+	$^1S_0$	0.761	2.173	2.186	2.151	2.160	1.822
5	2^+	$^3P_2$	0.814	0.846	0.856	0.803	0.805	0.926
6	3^+	$^3F_3$	1.254	1.280	1.302	1.190	1.195	1.378
7	1^+	$^2D_{3/2}\otimes{}^2S$	1.256	1.146	1.146	1.109	1.107	1.206
8	2^+	$^2D_{3/2}\otimes{}^2S$	1.673	1.868	1.874	1.814	1.812	
9	2^+	$^3F_2$	1.922	2.170	2.192	2.082	2.087	
10	0^+			3.037	3.039	3.034	3.037	
11	1^+	$^3P_1$	2.302	2.786	2.808	2.697	2.702	2.691
12	4^+	$^1G_4$	2.724	3.110	3.132	3.022	3.027	3.180
13	2^+	$^1D_2$	3.303	3.649	3.668	3.542	3.545	3.562
14	0^+			6.813	6.832	6.716	6.719	

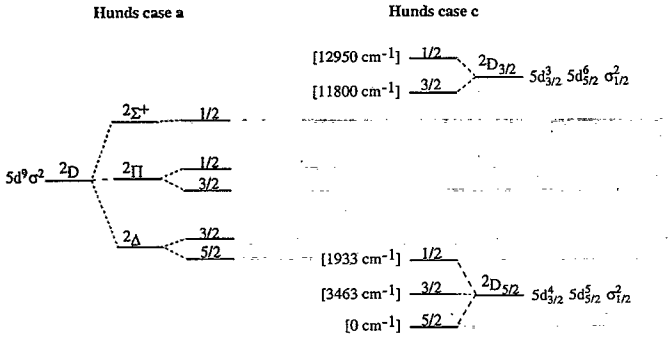

FIG. 1. Spectrum of PtH based on a *s-s* platinum–hydrogen bond arising from the Pt (d^9s^1) configuration. The figures in brackets are the excitation energies T_e obtained from the relativistic CI. Note the reordering of $\frac{3}{2}(1)$ and $\frac{1}{2}(1)$ states.

pling observed in platinum gives reason to expect considerable mixing between $^2\Sigma_{1/2}$ and $^2\Pi_{1/2}$, as well as between $^2\Pi_{3/2}$ and $^2\Delta_{3/2}$, thus making a Λ Σ assignment to the resulting states meaningless. We will therefore in general label the spinors with $\omega=|m_j|$ and the many-electron states with Ω (Hunds case c) and discuss bonding in PtH in terms of the latter bonding scheme.

A. Computational details

The molecular calculations were performed using C_{4v} double-group symmetry as our program package cannot exploit the full $C_{\infty v}$ double-group symmetry. In this symmetry $\omega=\frac{3}{2}, \frac{5}{2}$ spinors transform as the $E2$ representation, while the $\omega=\frac{1}{2}, \frac{7}{2}$ spinors transform as the $E1$ representation. At the DHF level the lowest three states [$\frac{1}{2}(1)$, $\frac{3}{2}(1)$ and $\frac{5}{2}(1)$] are described by one-determinantal wave functions with a hole in the highest $E1$ spinors, a hole in the second highest $E2$ spinors, or a hole in the highest $E2$ spinors, respectively. We have calculated the energies of the molecule at six distances from 1.5 to 1.6 Å. The energy of the separated atoms was calculated by taking the sum of the DHF platinum $J=3$ COSCI energy and the hydrogen energy calculated with our hydrogen basis. At three points the Gaunt interaction was calculated for the $\Omega=\frac{5}{2}$ and $\frac{1}{2}$ states as a perturbation after the SCF process.

Using the spinor set generated by the DHF calculations three separate CI calculations were performed at each Pt–H distance. One CI calculation was performed for $E1$ states using the $\Omega=\frac{1}{2}$ DHF wave function as reference, while the $\Omega=\frac{3}{2}$ and $\frac{5}{2}$ DHF wave functions were separate references in two CI calculations for $E2$ states. We put the ten occupied valence spinors into the RAS1 space, the two open valence spinors in RAS2 and 70 virtual spinors in RAS3. Virtual spinors with energies above 3.4 a.u. are deleted. All excitations from RAS1 to RAS2 are allowed, and single and double excitations from these spaces to RAS3 are allowed. This procedure is roughly equivalent to a multireference singles and doubles CI in which the reference consists of the six lowest twofold degenerate states. The resulting CI space consists of 535 932 determinants which is reduced by symmetry to 133 983 determinants for each component of the $E1$ and $E2$ representations. Only the Coulomb interaction was included in the two-electron integrals. Spectroscopic constants for PtH at the CI as well as the DHF level were obtained by fitting the potential curve to a Morse function. In accordance with the bonding scheme outlined above we used the platinum $J=3$ ($5d^9(^2D_{5/2})6s^1$) atomic asymptote for the lower three states and correspondingly the $J=1$ ($5d^9(^2D_{3/2})6s^1$) asymptote for the upper two states.

B. DHF results

The results from our DHF calculations are presented in Table V. The D_e values will be somewhat high since the atomic energies were based on an average spinor set while the molecular results were obtained by optimization of the separate states. The splitting between the lowest states is hardly affected by the Gaunt interaction. Hence, differential effects which are of importance for the atomic spectrum are of little significance for the molecular spectroscopic constants calculated. In our atomic calculations we found that the size of the Breit and Gaunt corrections is strongly dependent on the electronic configuration. As several configurations contribute to the lower states of the platinum atom one may expect differential effects of the Breit and Gaunt corrections on the atomic spectrum. The lack of corresponding differential effects on the three lower states of the PtH spectrum is then consistent with our assumption that all these states have a $5d^4_{3/2}5d^5_{5/2}\sigma^2_{1/2}$ configuration. Our molecular calculations further show insignificant differential effects of the Gaunt interaction on bond lengths and vibrational constants. This is consistent with previous calculations on hydride molecules[40] which showed that the differential effect of the Gaunt term is quite small and may be neglected for most molecular properties.

The spinors obtained from the DHF calculation can be analyzed by Mulliken population analysis[41] in much the

TABLE V. Molecular properties of PtH calculated by the DHF method. DHF+G refers to results obtained by the DHF method with the Gaunt correction added as a perturbation.

Method	State	r_e (Å)	D_e (eV)	ω_e (cm^{-1})	$\omega_e x_e$ (cm^{-1})	T_e (eV)
DHF	$\frac{5}{2}(1)$	1.548	2.28	2251	69	0.00
	$\frac{1}{2}(1)$	1.568	1.96	2095	70	0.32
	$\frac{3}{2}(1)$	1.581	1.86	2044	69	0.41
DHF+G	$\frac{5}{2}(1)$	1.549	2.32	2246	68	0.00
	$\frac{1}{2}(1)$	1.568	2.00	2095	68	0.31

TABLE VI. Valence density Mulliken population analysis of the DHF wave functions for the three lower states of PtH. Net charges are derived from total density.

ω	Occ.	Pt(s)	Pt(p)	Pt(d)	H(s)	H(p)	σ	π	δ
				$\Omega=\frac{5}{2}$; Pt net charge, 0.124					
$\frac{1}{2}$	6.0	1.161	0.068	3.655	1.097	0.013	4.005	1.994	0.000
$\frac{3}{2}$	4.0	0.000	0.000	3.994	0.000	0.000	0.000	2.000	2.000
$\frac{5}{2}$	hole	0.000	0.000	1.000	0.000	0.000	0.000	0.000	0.999
Sum	11.0	1.161	0.068	8.648	1.097	0.018	4.005	3.994	2.999
				$\Omega=\frac{1}{2}$; Pt net charge, 0.143					
$\frac{1}{2}$	4.0	0.412	0.071	2.421	1.080	0.012	2.301	1.698	0.000
	+hole	0.348	0.000	0.614	0.037	0.001	0.855	0.145	0.000
$\frac{3}{2}$	4.0	0.000	0.000	3.993	0.000	0.000	0.000	2.000	2.000
$\frac{5}{2}$	2.0	0.000	0.000	1.999	0.000	0.000	0.000	0.000	2.000
Sum	11.0	0.759	0.072	9.027	1.117	0.018	3.156	3.844	3.999
				$\Omega=\frac{3}{2}$; Pt net charge, 0.148					
$\frac{1}{2}$	6.0	1.102	0.071	1.842	1.123	0.015	4.008	1.991	0.000
$\frac{3}{2}$	2.0	0.000	0.000	1.997	0.000	0.001	0.000	0.856	1.144
	+hole	0.000	0.000	0.998	0.000	0.001	0.000	0.572	0.428
$\frac{5}{2}$	2.0	0.000	0.000	1.999	0.000	0.000	0.000	0.000	2.000
Sum	11.0	1.102	0.716	8.679	1.123	0.018	4.008	3.419	3.571

same way as nonrelativistic orbitals. Table VI shows the valence populations of the DHF wave functions in terms of the atomic basis functions. Conclusions based on a Mulliken population analysis should be viewed with caution as the analysis is basis dependent and the total energy is invariant to rotations among occupied spinors. An exception to this is the open-shell spinor that cannot be rotated into other spinors. Due to this property, the significant platinum s contribution (0.348) to the open-shell spinor for the $\frac{1}{2}(1)$ state is a clear indication of considerable d participation in the Pt–H bond. The total valence populations confirm that the dominant configuration of the platinum atom contributing to the molecule is d^9s^1. The d valence population is 9.0 for the $\frac{1}{2}(1)$ state, but somewhat smaller—about 8.7—for the $\frac{3}{2}(1)$ and $\frac{5}{2}(1)$ states. This may be taken as an indication of some contribution from the platinum d^8s^2 atomic configuration to the bonding in the latter two states. The platinum atom is found to have a small positive charge of about 0.13, which is in agreement with the other *ab initio* calculations. The density contribution of the small component basis functions (0.002 electron) is hardly noticeable at this scale.

The population analysis may also be set up in terms of the single group functions σ, π, and δ. These figures are also shown in Table VI and clearly illustrate the failure of the $\Lambda\Sigma$ coupling scheme. The $\Omega=\frac{5}{2}$ ground state may be described by the single $1\sigma^2 2\sigma^2 1\pi^4 1\delta^3$ configuration, but the $\Omega=\frac{1}{2}$ state is clearly not a pure $1\sigma^2 2\sigma^1 1\pi^4 1\delta^4$ configura-

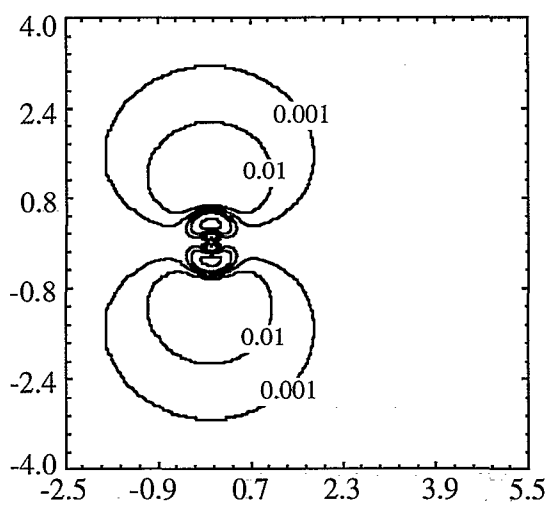

FIG. 2. Electron density plot of the $\omega=\frac{5}{2}$ open-shell spinor. Coordinates of the Pt atom are (0,0), coordinates of the H atom are (0,2.93). Figures in atomic units.

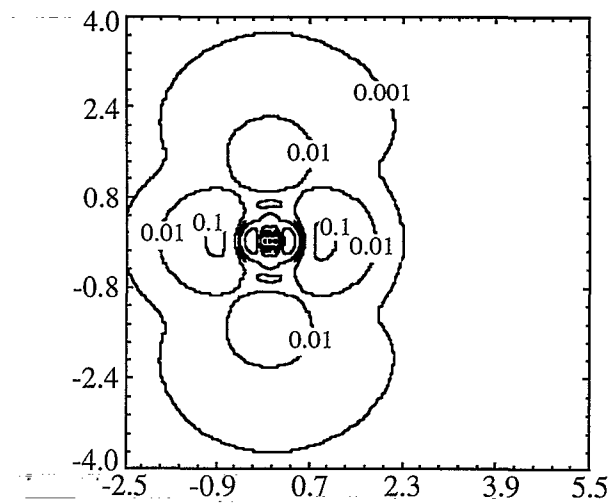

FIG. 3. Electron density plot of the $\omega=\frac{1}{2}$ open-shell spinor. Coordinates of the Pt atom are (0,0), coordinates of the H atom are (0,2.93). Figures in atomic units.

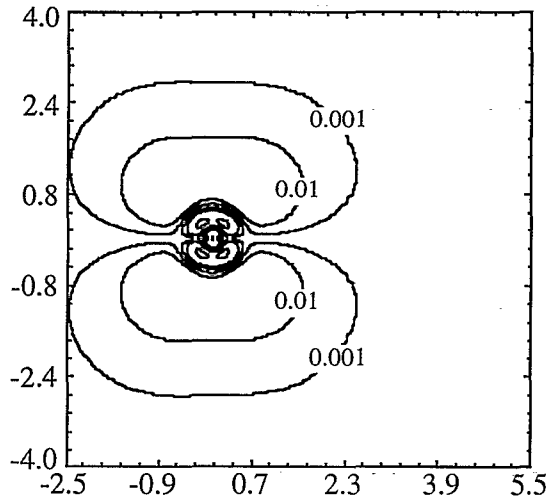

FIG. 4. Electron density plot of the $\omega=\frac{3}{2}$ open-shell spinor. Coordinates of the Pt atom are (0,0), coordinates of the H atom are (0,2.93). Figures in atomic units.

tion. In the $\Omega=\frac{3}{2}$ states the mixture of the $1\sigma^2 2\sigma^2 1\pi^3 1\delta^4$ and $1\sigma^2 2\sigma^2 1\pi^4 1\delta^3$ configurations is so strong (58% vs 42%) that the assignment to one of them is difficult. This strong mixing was also observed by Balasubramanian and Feng[6] and by Dyall.[8]

Another way of looking at the PtH electron distribution is by plotting the electron density. A plot of the total density will be dominated by the contribution of the platinum core electrons, and we have therefore plotted the density of open-shell spinors only for the three lower states (Figs. 2–4). The plots clearly show that the hole is located in a platinum d spinor.

C. CI results

The CI results are presented in Table VII. In the lower three states the weights of the DHF references are approximately 90% while other configurations contribute at most 0.4%. Static correlation is therefore not very important in the PtH molecule, as opposed to the platinum atom. The correlation energy is 258 mH for the $\frac{5}{2}(1)$ and $\frac{3}{2}(1)$ states and 261 mH for the $\frac{1}{2}(1)$. The somewhat larger correlation energy for the $\frac{1}{2}(1)$ state may be attributed to the larger valence d population of the corresponding reference. The effect on the electronic excitation spectrum is a small but significant reduction of the splitting between the $\frac{5}{2}(1)$ and $\frac{1}{2}(1)$ state. Correlation further shortens the bond lengths by 3–4 pm. Correlation f functions in the basis appear to be of importance, as was demonstrated by performing a small CI calculation on the $\frac{5}{2}(1)$ state in which 32 more virtual spinors, including the 14 nonbonding $5f$ spinors, were deleted from the active space. A three-point fit then gave a bond length of 1.544 Å as compared with 1.518 Å obtained with the larger CI. From the bond shortening and the enlargement of D_e and ω_e one can conclude that the bond is stronger than would be expected on basis of the DHF results. The gap between the lower three and the upper two states is about the same magnitude as the spin–orbit splitting in the platinum d shell (Table IV).

TABLE VII. Molecular properties of PtH calculated by the relativistic CI method.

State	r_e (Å)	D_e (eV)	ω_e (cm^{-1})	$\omega_e x_e$ (cm^{-1})	T_e (eV)
$\frac{5}{2}(1)$	1.518	2.98	2458	63	0.00
$\frac{1}{2}(1)$	1.526	2.74	2419	66	0.24
$\frac{3}{2}(1)$	1.542	2.54	2313	65	0.44
$\frac{3}{2}(2)$	1.540	2.73	2365	62	1.46
$\frac{1}{2}(2)$	1.562	2.58	2277	64	1.61

TABLE VIII. Excitation energies T_e (eV) for $\Lambda\Sigma$ states calculated by different methods.

	RECP			All electron	
State	MP4[a]	MRSDCI[b]	MRSDCI[c]	CASSCF[d]	MRSDCI[e]
$^2\Sigma$	0.00	0.00	0.00	0.00	0.00
$^2\Delta$	−0.16	−0.05	0.34	−0.09	0.09
$^2\Pi$	0.52	0.69	0.69	0.50	0.73

[a]Rohlfing *et al.* (Ref. 4): RECP-UHF-MP4.
[b]Balasubramanian and Feng (Ref. 6): RECP-CASSCF-MRSDCI.
[c]Gropen *et al.* (Ref. 7): RECP-CASSCF-MRSDCI.
[d]Gropen (Ref. 43): All-electron CASSCF using the second-order Douglas–Kroll approximation.
[e]Gropen (Ref. 43): All-electron CASSCF-MRSDCI using the second-order Douglas–Kroll approximation.

V. DISCUSSION

Our CI as well as DHF results fit within the relativistic bonding scheme outlined above in which the electronic configuration of the three lower and two upper states of PtH may be written as $5d^4_{3/2}5d^5_{5/2}\sigma^2_{1/2}$ and $5d^3_{3/2}5d^6_{5/2}\sigma^2_{1/2}$, respectively. The assigned configurations are only approximate and are perturbed by $5d$ participation in bonding that changes the order of the three lower states from the expected $\frac{5}{2}(1)<\frac{3}{2}(1)<\frac{1}{2}(1)$ sequence to $\frac{5}{2}(1)<\frac{1}{2}(1)<\frac{3}{2}(1)$. Further confirmation of the bonding scheme stems from the DHF results of Dyall.[8] Dyall performed DHF calculations on the five lower states of PtH using a $9s8p7d3f$ contracted Gaussian large component basis for platinum derived from the same primitive Gaussian basis (basis I) as our contracted Pt basis (basis II). The lowest three PtH states were analyzed by Dyall to be mainly $d_{5/2}$ hole states while the upper two are essentially $d_{3/2}$ hole states.

Most *ab initio* calculations on PtH, however, employ spin-free RECP's and optimize the $\Lambda\Sigma$-states ($^2\Delta$, $^2\Pi$, and $^2\Sigma$) as a first stage. In Table VIII we list some results obtained for the $\Lambda\Sigma$ states. Rohlfing *et al.*[4] used a RECP obtained from the Cowan–Griffin method[12] and a $5s5p3d1f$ uncontracted Gaussian valence basis. They did unrestricted Hartree–Fock (UHF) calculations and then introduced electron correlation through fourth order Møller–Plesset perturbation theory [MP4(SDTQ)]. Balasubramanian and Feng,[6] using a j averaged RECP fitted to numerical atomic DHF calculations and a $3s2p3d$ contracted Gaussian valence basis, performed a small complete active space SCF (CASSCF) calculation with 11

TABLE IX. Comparison of excitation energies T_e (in eV) for states of PtH obtained by different methods.

	RECP			All-electron				
State	MP4[a]	SDCI[b]	SDCI[c]	SDCI[d]	DHF[e]	DHF[f]	Rel. CI[f]	Expt.[g]
$\frac{5}{2}(1)$	0.00	0.00	0.00	0.00	0.00	0.00	0.00	0.00
$\frac{1}{2}(1)$	0.31	0.19	0.19	0.11	0.34	0.32	0.24	
$\frac{3}{2}(1)$	0.45	0.52	0.45	0.44	0.42	0.41	0.44	0.41
$\frac{5}{2}(2)$	1.28	1.35	1.29	1.37	1.43		1.46	1.45
$\frac{1}{2}(2)$	1.57	1.35	1.55	1.61	1.55		1.61	

[a]Rohlfing *et al.* (Ref. 4): RECP-UHF-MP4+spin–orbit (semiempirically) (A=0.418 eV).
[b]Balasubramanian and Feng (Ref. 6): RECP-CASSCF-MRSDCI+spin–orbit (RECP).
[c]Gropen (Ref. 7): RECP-CASSCF-MRSDCI+spin–orbit (semiempirically) (A=0.418 eV).
[d]Gropen (Ref. 43): All-electron CASSCF-MRSDCI using the second-order Douglas–Kroll approximation +spin–orbit (A=0.467 eV).
[e]Dyall (Ref. 8): DHF.
[f]Present work.
[g]McCarthy *et al.* (Ref. 47).

electrons in an active space of 14 spin orbitals. They then did multireference singles CI (MRSCI) to determine potential surfaces and multireference singles plus doubles CI (MRSDCI) to determine dissociation and excitation energies at the optimized geometries. At the singles level the $^2\Delta$ state is 0.12 eV above the $^2\Sigma$ state, while the order is reversed at the MRSDCI level with $^2\Delta$ as the ground state. Gropen *et al.*[7] obtained their RECP from an atomic calculation using the second order Douglas–Kroll approximation[13] and employed a $3s3p4d2f$ contracted Gaussian valence basis. They did a CASSCF calculation with 11 electrons in an active space of 14 spin orbitals followed by MRSDCI. Their article contains an error as the $^2\Sigma$ state at the CASSCF level is 0.04 eV above and not 0.34 eV below the $^2\Delta$ state, the latter being the MRSDCI result.

The results obtained for the $\Lambda\Sigma$ states and listed in Table VIII vary considerably and it is difficult to assess to what extent this spread may be related to the correlation treatment or to the quality of basis sets or the RECP's. The RECP used by Wang and Pitzer[3] was fitted to a j-averaged atomic DHF calculation and appears to be too repulsive as the resulting bond lengths and spectrum deviate markedly from all other results. Clearly, there is a need for an all-electron molecular calibration calculation at this level of approximation. Gropen[42] has recently performed an all-electron CASSCF-MRSDCI using the second-order Douglas–Kroll approximation[13] and a $8s7p5d3f$ contracted Gaussian basis. Preliminary results from CASSCF as well as MRSDCI calculations at 1.55 Å are included in Table VIII. The results indicate that the $^2\Delta$ and $^2\Sigma$ states are near degenerate, but that correlation tends to favor $^2\Sigma$ as ground state.

Spin–orbit interaction is introduced in the RECP calculations through various perturbational schemes. Balasubramanian and Feng[6] add spin–orbit matrix elements to their CI matrix. The spin–orbit matrix elements were derived from the RECP (Ref. 43) and thus depend on the quality of the potential. Rohlfing *et al.*[4] introduce spin–orbit splitting semiempirically. To the diagonal matrix of electronic energies of the $\Lambda\Sigma$ states they add a spin–orbit matrix for the separated atoms using an atomic spin–orbit parameter derived from experiment. They do not state exactly what parameter value they used, but it appears to be the parameter A=0.418 eV derived from the splitting of the platinum positive ion d^9 state.[44] The approach of Gropen *et al.*[7] is quite similar, but neglects off-diagonal matrix elements.

Experimental data on the PtH molecule are scarce and restricted to the $\frac{3}{2}$ and $\frac{5}{2}$ states. Most experimental work has been done by the group of Scullman,[45] but one may also mention the early study by Loginov.[46] Recently McCarthy *et al.*[47] reported laser excitation and Fourier transform spectroscopic results which give more precise estimates of $\frac{5}{2}(1)\rightarrow\frac{3}{2}(1)$ and $\frac{3}{2}(1)$-$\frac{5}{2}(1)\rightarrow\frac{3}{2}(2)$ excitation energies. They also note a reversal of parity in the Ω doubling for vibronic states at the $\frac{3}{2}(2)$ level and attribute this to the $\frac{1}{2}(2)$ state being above and pushing down on $\frac{3}{2}(2)$ vibronic states. This is the only experimental indication so far of the position of $\Omega=\frac{1}{2}$ states in the PtH spectrum. The possible $\frac{1}{2}$-$\frac{1}{2}$ transition reported by Scullman was later shown to be caused by a gold impurity.[48] The experimental studies indicate an unusual stability of the Pt–H bond. The experimental value of 3.6±0.4 eV obtained by Birge–Sponer extrapolation is the largest measured bond energy of any transition metal hydride.[49]

Table IX lists excitation energies T_e and Table X bondlengths r_e and harmonic frequencies ω_e obtained from a number of studies of PtH. Experimental excitation energies T_e were deduced from the corresponding T_0 values using the formula $T_e=T_0^0+\frac{1}{2}\Delta\omega_e-\frac{1}{4}\Delta\omega_e x_e$. The relativistic CI gives the best overall agreement with experiment for these properties. Since our relativistic CI results should be better than our DHF results, agreement on the DHF level with the $\frac{5}{2}(1)$-$\frac{3}{2}(1)$ splitting is probably somewhat coincidental. The good agreement between our DHF results and those of Dyall[8] should also be noted. The differences in r_e are smaller than 0.005 Å while the excitation energies differs by at most 0.02 eV. This indicates that basis set errors in the two calculations are of equal size.

The excitation energies calculated by Balasubramanian and Feng[6] agree rather well with our CI results, although their two upper states appear rather low indicating that

TABLE X. Bondlengths r_e (in Å) of PtH calculated by different methods. Corresponding harmonic frequencies ω_e (in cm^{-1}) are given in parentheses.

State	MRSCI[a]	DHF[b]	DHF[c]	Rel. CI[c]	Experiment[d]
$\frac{5}{2}$ (1)	1.55 (2177)	1.551 (2234)	1.548 (2251)	1.518 (2458)	1.528 (2378)
$\frac{1}{2}$ (1)	1.54 (2188)	1.573 (2094)	1.568 (2095)	1.526 (2419)	
$\frac{3}{2}$ (1)	1.58 (2155)	1.584 (2080)	1.581 (2044)	1.542 (2313)	1.520 (2265)
$\frac{3}{2}$ (2)	1.59 (2179)	1.577 (2162)		1.540 (2359)	(2349)[e]
$\frac{1}{2}$ (2)	1.58 (2021)	1.590 (2097)		1.562 (2225)	

[a]Balasubramanian and Feng (Ref. 6): RECP-CASSCF-MRSCI+spin–orbit (RECP).
[b]Dyall (Ref. 8): DHF.
[c]Present work.
[d]Scullman *et al.* (Ref. 45).
[e]Calculated using the formula $\omega_e = \Delta G_{1/2} - 2\omega_e x_e$, in which the $\Delta G_{1/2}$ value obtained by McCarthy *et al.* (Ref. 47) and our calculated value for $\omega_e x_e$ were used.

spin–orbit splitting is somewhat underestimated. Their calculated bond lengths are appreciable longer and harmonic frequencies smaller than ours, a feature that is probably explained by insufficient correlation particularly due to their lack of correlating f functions. The neglect of off-diagonal spin–orbit matrix elements by Gropen *et al.*[7] is hardly justifiable on the basis of the strong mixing of $\Lambda\Sigma$ states through the spin–orbit interaction. We have therefore recalculated the spin–orbit splitting from their results using the semiempirical method of Rohlfing *et al.*[4] The results obtained using this semiempirical method agree rather well with our CI results and indicate that platinum retains much of its atomic character in PtH. This is in accordance with our bonding model and justifies the assignment of the $5d^4_{3/2}5d^5_{5/2}\sigma^2_{1/2}$ and $5d^3_{3/2}5d^6_{5/2}\sigma^2_{1/2}$ electronic configuration for the three lower and two upper states of PtH respectively. The electronic configurations invites a comparison with the d^9s^2 negative platinum ion and indicates an analogy between the binding of an electron and of a hydrogen atom to platinum. Squires[49] has investigated the possible correlation of transition-metal electron affinity EA(M) and the dissociation energy $D[M–H]$ of the corresponding transition metal hydride. The study was motivated by the near constant gas-phase acidity observed for these hydrides. Squires obtains an empirical formula linking the two above quantities ($D[M–H]$=EA(M)+1.19 eV). The electron affinity of platinum is 2.13 eV which is almost twice the corresponding value for nickel (1.16 eV).[50] The much larger value for platinum can be understood in terms of relativistic stabilization of the 6s orbital.[10] The unusual stability of the Pt–H bond may then be explained in an analogous fashion.

The analogy between the PtH molecule and the Pt negative ion further suggests that the spin–orbit parameter of the semiempirical method used by Rohlfing *et al.*[4] should be derived from the fine structure splitting of the negative rather than the positive platinum ion. Both the negative ion and the PtH molecule can be well represented with a single configurational (d^9s^2 or $d^9\sigma^2$) wave function. In the positive ion the contribution of the d^8s configuration is non-negligble and decreases the spin–orbit coupling. The use of a spin–orbit parameter that was derived from the Pt^+ experimental splitting will thus underestimate the splitting in the molecule. A better choice is to obtain the spin–orbit parameter either from an experiment or calculation on the negative ion or from a calculation on Pt^+ that includes only the d^9 configuration. Unfortunately, the $^2D_{5/2}$–$^2D_{3/2}$ splitting of the d^9s^2 negative platinum ion has not been experimentally determined. The recommended value[51] 10 000 ($\pm$1000) cm^{-1} obtained by isoelectronic extrapolation gives a spin–orbit parameter A=0.50 eV from the Landé interval rule. Numerical calculations on the d^9, d^9s, and d^9s^2 configurations of Pt^+, Pt, and Pt^- give values for A of 0.49, 0.50, and 0.47 eV, respectively. We have used the latter value to obtain spin–orbit splitted excitations energies from the preliminary all-electron CASSCF-MRSDCI results of Gropen.[42] The results are listed in Table IX and agree well with our CI results.

VI. CONCLUSIONS

The electronic structure and bonding of the five lower states of the PtH molecule have been investigated using fully relativistic CI based on DHF references. Spectroscopic properties have been obtained by fitting of a Morse potential tending asymptotically to the Pt[J=3($5d^9(^2D_{5/2})6s^1$)]+H($6s^1$) and Pt[J=($5d^9(^2D_{3/2})6s^1$)]+H($6s^1$) energies for the three lower and two upper states respectively. At the DHF level the effect of relativistic corrections (Gaunt interaction) to the Coulomb electron–electron interaction has been evaluated and found to be hardly significant for the properties mentioned above. At the CI level the wave functions are found to have only one dominant configuration. This indicates a lack of static correlation and is quite contrary to the results obtained for the platinum atom. Dynamic correlation in the d shell is important for the spectroscopic properties of PtH and the inclusion of correlating f functions in the basis appears to give considerable improvement of the results.

Our CI, as well as DHF results, indicate that bonding is essentially the same in all five states of PtH. The results are in accordance with a bonding scheme in which the electronic configuration of the three lower and two upper states of PtH are assigned the electronic configurations $5d^4_{3/2}5d^5_{5/2}\sigma^2_{1/2}$ and $5d^3_{3/2}5d^6_{5/2}\sigma^2_{1/2}$, respectively. The ground state of the PtH molecule is found to be an $\Omega=\frac{5}{2}$ state strongly bound with a D_e value of 2.98 eV and a bondlength of 1.52 Å. The assigned electronic configura-

TABLE XI. The hydrogen basis set.

	Exponents	Contraction coefficients		
		Large components		
s	79.990 16053	0.002 093 89	−0.009 769 42	−0.002 895 11
	11.964 35285	0.016 078 26	−0.075 016 06	−0.022 230 54
	2.722 56964	0.078 682 58	−0.367 107 84	−0.108 790 11
	0.772 82765	0.263 230 87	−1.228 151 36	−0.363 954 98
	0.251 76829	0.497 096 74	2.452 348 58	−0.835 626 69
	0.088 42324	0.286 271 56	−1.335 651 87	1.430 315 43
p	0.800 00000	1.000 000 00		
		Small components		
s	0.800 000 00	1.000 000 00		
p	79.990 160 53	0.032 425 34	−0.0573 3506	0.006 956 49
	11.964 352 85	0.096 320 89	−0.1702 5340	0.020 691 24
	2.722 569 64	0.224 873 92	−0.3974 3861	0.048 323 67
	0.772 827 65	0.400 833 34	−0.7083 9556	0.086 149 12
	0.251 768 29	0.432 049 06	1.2670 4631	−1.139 460 20
	0.088 423 24	0.147 453 73	−0.2605 8929	1.482 128 54
d	0.800 000 00	1.000 000 00		

tions suggest an analogy between the PtH molecule and the platinum d^9s^2 negative ion. The stability of the Pt–H bond may then be explained by the relativistic stabilization of the platinum 6*s* orbital. The strong atomic character of platinum in the molecule may explain the success of more approximative approaches to the spin–orbit splitted states of PtH. On the basis of the analogy with the negative Pt ion we recommend the use of a spin–orbit parameter that is derived from the spin–orbit splitting of the negative Pt ion in the semiempirical approach used by Rohlfing *et al.*[4] The results show good agreement with experimental data and illustrate the value of four-component relativistic CI calculations to provide accurate benchmark results for systems in which both relativistic and correlation effects are important.

ACKNOWLEDGMENTS

The authors would like to thank K. Dyall, L. Veseth, and K. Balasubramanian for discussions and comments. Thanks are also due to Roar Skaalin and Arve Dispen at SINTEF, Norway, for technical assistance in the computations performed on the National CRAY Y/MP Supercomputer. Grants of computing time from the Norwegian Supercomputing Committee (TRU) and from the Netherlands National Computing Facilities Foundation (NCF) are gratefully acknowledged. Luuk Visscher is supported by the Netherlands Foundation for Fundamental Research on Matter (FOM) with financial aid from the Netherlands Organisation for Scientific Research (NWO). Trond Saue is supported by a grant from the Norwegian Research Council for Sciences and the Humanities (NAVF).

APPENDIX A: HYDROGEN BASIS

The hydrogen basis used in the calculations was derived from a 6*s*1*p* primitive basis and contracted to 3*s*1*p*. The basis is given in Table XI.

[1] F. R. Hartley, *Chemistry of the Platinum Group Metals* (Elsevier, Amsterdam, 1991).
[2] H. Basch and S. Topiol, J. Chem. Phys. **71**, 802 (1979).
[3] S. W. Wang and K. S. Pitzer, J. Chem. Phys. **79**, 3851 (1983).
[4] C. M. Rohlfing, P. J. Hay, and R. L. Martin, J. Chem. Phys. **85**, 1447 (1986).
[5] G. Rasch and S. Tobisch, Chem. Phys. Lett. **166**, 311 (1990).
[6] K. Balasubramanian and P. Y. Feng, J. Chem. Phys. **92**, 541 (1990).
[7] O. Gropen, J. Almlöf, and U. Wahlgren, J. Chem. Phys. **96**, 8363 (1992).
[8] K. Dyall, J. Chem. Phys. **98**, 9678 (1993).
[9] S. R. Langhoff and C. W. Bauschlicher, Ann. Rev. Phys. Chem. **39**, 181 (1988).
[10] P. Pyykkö, Chem. Rev. **8**, 563 (1988).
[11] O. Gropen, in *Methods of Computational Chemistry*, edited by S. Wilson (Plenum, New York, 1988), Vol. 2, p. 1.
[12] R. D. Cowan and D. C. Griffin, J. Opt. Soc. Am. **66**, 1010 (1976).
[13] M. Douglas and N. M. Kroll, Ann. Phys. (N.Y.) **82**, 89 (1974).
[14] G. Malli and J. Oreg, J. Chem. Phys. **63**, 830 (1975).
[15] P. J. C. Aerts and W. C. Nieuwpoort, Proceedings of the 6th Seminar on Computational Methods in Quantum Chemistry, Schloss Ringberg (Tegernsee), September 4–7, 1984 (unpublished).
[16] S. Okada and O. Matsuoka, J. Chem. Phys. **91**, 4193 (1989).
[17] K. G. Dyall, K. Fægri, Jr., and P. R. Taylor, in *The Effects of Relativity in Atoms, Molecules and the Solid State*, edited by I. P. Grant, B. Gyorffy, and S. Wilson (Plenum, New York, 1991).
[18] A. K. Mohanty and E. Clementi, Int. J. Quantum Chem. **39**, 487 (1990).
[19] T. Saue, Ph.D. thesis, University of Oslo, 1991 (unpublished).
[20] L. Visscher, Ph.D. thesis, University of Groningen, 1993. MOLFDIR is scheduled to be available in the MOTECC'94 suite of programs.
[21] R. E. Moss, *Advanced Molecular Quantum Mechanics* (Benjamin, London, 1968).
[22] M. E. Rose, *Relativistic Electron Theory* (Wiley, New York, 1961).
[23] G. Breit, Phys. Rev. **34**, 553 (1929).
[24] Y.-K. Kim, Phys. Rev. **154**, 17 (1967).
[25] J. A. Gaunt, Proc. R. Soc. (London) Ser. A **122**, 513 (1929).
[26] C. C. J. Roothaan, Rev. Mod. Phys. **32**, 179 (1960).
[27] L. Visscher, P. J. C. Aerts, and O. Visser, in *The Effects of Relativity in Atoms, Molecules and the Solid State*, edited by S. Wilson, I. P. Grant, and B. Gyorffy (Plenum, New York, 1991).
[28] O. Visser, L. Visscher, P. J. C. Aerts, and W. C. Nieuwpoort, J. Chem. Phys. **96**, 2910 (1992).
[29] J. Olsen, B. O. Roos, P. Jørgensen, and H. J. Aa. Jensen, J. Chem. Phys. **89**, 2185 (1988).
[30] E. R. Davidson, J. Comput. Phys. **17**, 87 (1975).
[31] C. E. Moore, Natl. Bur. Stand. (U.S.) Circ. No. 467 (U.S. GPO, Washington, D.C., 1958), Vol. 181.

[32] K. G. Dyall, I. P. Grant, C. T. Johnson, E. P. Plummer, and F. Parpia, Comput. Phys. Commun. **50**, 375 (1989). Basis set extension: K. G. Dyall, K. Fægri, P. R. Taylor, and H. Partridge, J. Chem. Phys. **95**, 2583 (1991).
[33] K. Fægri, Theoretical Chemistry, University of Oslo, Technical Note, June 1987 (unpublished).
[34] O. Matsuoka and S. Okada, Chem. Phys. Lett. **155**, 547 (1989).
[35] O. Visser, P. J. C. Aerts, D. Hegarty, and W. C. Nieuwpoort, Chem. Phys. Lett. **134**, 34 (1987).
[36] O. Gropen, M. Sjøvoll, H. Strømsnes, E. Karlsen, O. Swang, and K. Fægri, Theo. Chim. Acta (to be published).
[37] L. Visscher, P. J. C. Aerts, O. Visser, and W. C. Nieuwpoort, Int. J. Quantum Chem. **25**, 131 (1991).
[38] P. J. Hay, J. Chem. Phys. **66**, 4377–84 (1977).
[39] R. S. Mulliken, Rev. Mod. Phys. **4**, 1 (1932).
[40] O. Visser, L. Visscher, P. J. C. Aerts, and W. C. Nieuwpoort, Theo. Chim. Acta **81**, 405 (1992).
[41] R. Mulliken, J. Chem. Phys. **23**, 1833 (1955).
[42] O. Gropen, Int. J. Quantum. Chem. (to be published).
[43] K. S. Pitzer, Int. J. Quantum Chem. **25**, 131 (1984).
[44] This assumption is supported by the fact that a recalculation by C. Marian (private communication) using this parameter gives exactly the same excitation energies.
[45] H. Neuhaus and R. Scullman, Z. Naturforsch. A **19**, 659 (1964); R. Scullman, Ark. Fys. **28**, 255 (1964); B. Kaving and R. Scullman, Can. J. Phys. **49**, 2264 (1971); B. Kaving and R. Scullman, Phys. Scr. **9**, 33 (1974); R. Scullman and P. Cederbalk, J. Phys. B **10**, 3659 (1977); G. Gustafsson and R. Scullman, Mol. Phys. **67**, 981 (1989).
[46] V. A. Loginov, Opt. Spectrosc. (USSR) **20**, 88 (1966).
[47] M. C. McCarthy, R. W. Field, R. Engleman, Jr., and P. F. Bernath, J. Mol. Spectrosc. **158**, 208 (1993).
[48] R. Scullman (private communication).
[49] R. R. Squires, J. Am. Chem. Soc. **107**, 4385 (1985).
[50] R. D. Mead, A. E. Stevens, and W. C. Lineberger, in *Gas Phase Ion Chemistry*, edited by M. T. Bowers (Academic, New York, 1984), Vol. 3, Chap. 22.
[51] H. Hotop and W. C. Lineberger, J. Phys. Chem. Ref. Data **4**, 539 (1975).